Reaction Mechanisms for C−O Bond Coupling from Pt 4CH2+ and O2 : A Relativistic Density Functional Study

ARTICLE *in* ORGANOMETALLICS · MAY 2008

Impact Factor: 4.13 · DOI: 10.1021/om700288a

2 AUTHORS:

Fei Xia
East China Normal University
35 PUBLICATIONS **211** CITATIONS
SEE PROFILE

Zexing Cao
Xiamen University
183 PUBLICATIONS **2,097** CITATIONS
SEE PROFILE

Reaction Mechanisms for C−O Bond Coupling from $Pt_4CH_2^+$ and O_2: A Relativistic Density Functional Study

Fei Xia and Zexing Cao*

Department of Chemistry and State Key Laboratory of Physical Chemistry of Solid Surfaces, Xiamen University, Xiamen 361005, China

Received March 26, 2007

Computational investigations on the reaction of $Pt_4CH_2^+$ with O_2 have been carried out by the relativistic density functional approach. Calculations indicate that the reactivity of $Pt_4CH_2^+$ toward O_2 is different from the metallic carbene $PtCH_2^+$. The dehydrogenation route in the reaction of $Pt_4CH_2^+$ with O_2 is quite unfavorable, both dynamically and thermodynamically. The reaction channels to products H_2O/CO and HCOOH with involvement of O−O bond activation and C−O bond coupling are strikingly exothermic, where the C−O bond coupling and the release of CO are the crucial steps for the entire reaction channels. Predicted overall Gibbs free energies of reaction ΔG are −66.2 kcal mol^{-1} for H_2O/CO and −73.5 kcal mol^{-1} for HCOOH, respectively. Both energy-favored routes have thus relatively high reaction efficiencies toward O_2 in comparison with dehydrogenation. On the basis of theoretical results, plausible mechanisms for the reaction of $Pt_4CH_2^+$ with O_2 and candidates for the experimental neutral products [C, H_2, O_2] in reaction have been proposed.

1. Introduction

The transition-metal platinum plays a vital role in methane functionalization due to its significant reactivity toward methane activation.[1] In general, the methane functionalization by the gaseous platinum clusters mainly consists of two essential processes: first, the dehydrogenation of methane yields the metallic carbene species; second, the resultant carbene species consecutively reacts with the substrates, such as dioxygen, ammonia, or other small molecules, to generate ultimate key products.[2]

The transition-metal cationic clusters Pt_n^+ ($n = 1-24$) have been found to be quite reactive for methane dehydrogenation in the gas phase.[3] Among the bare platinum clusters, the reaction of bare Pt^+ with CH_4 has been extensively investigated by experiments in combination with theoretical calculations.[4,5] The resultant carbene species $PtCH_2^+$ from methane dehydrogenation has been served as the key precursor to subsequent reactions in methane functionalization.[6] Experimental studies by Wesendrup et al.[7] show that the metallic carbene species $PtCH_2^+$ can react with O_2 to yield methanol, formaldehyde, and other oxygen-containing products in the catalytic cycle mediated by Pt^+. Aschi et al.[8] also have set up a gap-phase model of the reaction of $PtCH_2^+$ with NH_3 for the synthesis of hydrogen cyanide in the heterogeneous process. Such reactions are usually classified into the category of the carbon−heteroatom bond coupling reaction.[9,10] Chemical syntheses of methanol, formaldehyde, and formic acid are inevitably involved with this bond coupling process.

Theoretical investigations of potential energy surfaces for the platinum-mediated reactions are still challenging in accuracy due to its remarkable relativistic effects. Pavlov et al.[4b] have qualitatively computed the potential energy surfaces of reactions of $PtCH_2^+$ with O_2 in detail. They discussed possible reaction mechanisms and proposed different candidates for observed

* To whom correspondence should be addressed. E-mail: zxcao@xmu.edu.cn.

(1) (a) Martinho Simöes, J. A.; Beauchamp, J. L. *Chem. Rev.* **1990**, *90*, 629. (b) Eller, K.; Schwarz, H. *Chem. Rev.* **1991**, *91*, 1121. (c) Schwarz, H. *Angew. Chem., Int. Ed. Engl.* **1991**, *30*, 820. (d) Weisshaar, J. C. *Acc. Chem. Res.* **1993**, *26*, 213. (e) Lersch, M.; Tilset, M. *Chem. Rev.* **2005**, *105*, 2471.

(2) (a) Trevor, D. J.; Cox, D. M.; Kaldor, A. *J. Am. Chem. Soc.* **1989**, *112*, 3742. (b) Kaldor, D. A.; Cox, D. M. *Pure Appl. Chem.* **1990**, *62*, 79. (c) Irikura, K. K.; Beauchamp, J. L. *J. Am. Chem. Soc.* **1991**, *113*, 2769. (d) Irikura, K. K.; Beauchamp, J. L. *J. Phys. Chem.* **1991**, *95*, 8344. (e) Carroll, J. J.; Weisshaar, J. C.; Siegbahn, P. E. M.; Wittborn, C. A. M.; Blomberg, M. R. A. *J. Phys. Chem.* **1996**, *99*, 14388. (f) Achatz, U.; Beyer, M.; Joos, S.; Fox, B. S.; Niedner-Schatteburg, G.; Bondybey, V. E. *J. Phys. Chem. A* **1999**, *103*, 8200. (g) Schwarz, H.; Schröder, D. *Pure Appl. Chem.* **2000**, *72*, 2319. (h) Zhang, X. G.; Liyanage, R.; Armentrout, P. B. *J. Am. Chem. Soc.* **2001**, *123*, 5563. (i) Koszinowski, K.; Schröder, D.; Schwarz, H. *ChemPhysChem* **2003**, *4*, 1233.

(3) (a) Achatz, U.; Berg, C.; Joos, S.; Fox, B. S.; Beyer, M. K.; Niedner-Schatteburg, G.; Bondybey, V. E. *Chem. Phys. Lett.* **2000**, *320*, 53. (b) Koszinowski, K.; Schröder, D.; Schwarz, H. *J. Phys. Chem. A* **2003**, *107*, 4999. (c) Kummerlöwe, G.; Balteanu, I.; Sun, Z.; Balaj, O. P.; Bondybey, V. E.; Beyer, M. K. *Int. J. Mass Spectrom.* **2006**, *254*, 183. (d) Adlhart, C.; Uggerud, E. *Chem. Comm.* **2006**, *24*, 2581.

(4) (a) Heinemann, C.; Wesendrup, R.; Schwarz, H. *Chem. Phys. Lett.* **1995**, *239*, 75. (b) Pavlov, M.; Blomberg, M. R. A.; Siegbahn, P. E. M.; Wesendrup, R.; Heinemann, C.; Schwarz, H. *J. Phys. Chem. A* **1997**, *101*, 1567.

(5) (a) Cui, Q.; Musaev, D. G.; Morokuma, K. *J. Chem. Phys.* **1998**, *180*, 8418. (b) Cui, Q.; Musaev, D. G.; Morokuma, K. *J. Phys. Chem. A* **1998**, *102*, 6373. (c) Xia, F.; Cao, Z. X. *J. Phys. Chem. A* **2006**, *110*, 10078. (d) Xiao, L.; Wang, L. C. *J. Phys. Chem. B* **2007**, *111*, 1657.

(6) (a) Heinemann, C.; Hertwig, R.; Wesendrup, R.; Koch, W.; Schwarz, H. *J. Am. Chem. Soc.* **1995**, *117*, 495. (b) Heinemann, C.; Schwarz, H.; Koch, W.; Dyall, K. G. *J. Chem. Phys.* **1996**, *104*, 4642. (c) Rakowitz, F.; Marian, C. M.; Schimmelpfennig, B. *Phys. Chem. Chem. Phys.* **2000**, *2*, 2481.

(7) Wesendrup, R.; Schröder, D.; Schwarz, H. *Angew. Chem., Int. Ed. Engl.* **1994**, *33*, 1174.

(8) Aschi, M.; Brönstrup, M.; Diefenbash, M.; Harvey, J. N.; Schröder, D.; Schwarz, H. *Angew. Chem., Int. Ed.* **1998**, *37*, 829.

(9) Koszinowski, K.; Schröder, D.; Schwarz, H. *Organometallics* **2003**, *22*, 3809.

(10) (a) Bröstrup, M.; Schröder, D.; Schwarz, H. *Organometallics* **1999**, *18*, 1939. (b) Koszinowski, K.; Schröder, D.; Schwarz, H. *J. Am. Chem. Soc.* **2003**, *125*, 3670. (c) Koszinowski, K.; Schröder, D.; Schwarz, H. *Angew. Chem., Int. Ed.* **2004**, *43*, 121. (d) Koszinowski, K.; Schröder, D.; Schwarz, H. *Organometallics* **2004**, *23*, 1132. (e) Böhme, D. K.; Schwarz, H. *Angew. Chem., Int. Ed.* **2005**, *44*, 2336. (f) Xia, F.; Chen, J.; Zeng, K.; Cao, Z. X. *Organometallic* **2005**, *24*, 1845. (g) Xia, F.; Chen, J.; Cao, Z. X. *Chem. Phys. Lett.* **2006**, *418*, 386.

10.1021/om700288a CCC: $37.00
Publication on Web 10/25/2007

neutral products [C, H_2, O_2] in experiments, namely, H_2/CO_2, H_2O/CO, or HCOOH.[9]

Among the reactions induced by $PtCH_2^+$, the most fascinating one is the functionalization reaction of $PtCH_2^+$ with O_2, where the formic acid presumably exists in the products. Furthermore, the experimental studies reveal that the reactivity of species $Pt_nCH_2^+$ ($n = 2-4$) with O_2 depends on the cluster size. For example, the measured reaction efficiency of $PtCH_2^+$ is 0.028 while that of $Pt_4CH_2^+$ is 0.17, much more efficient than the former.[9] In the C−N bond coupling, the carbene species $PtCH_2^+$ reacting with NH_3 may result in three different products, whereas the clusters $Pt_nCH_2^+$ ($n \geq 2$) exclusively dehydrogenate the CH_2 moiety.[10]

Such striking size dependence of reactivity and catalytic reaction routes for the platinum cluster cations stimulates our interest to investigate the reaction mechanisms of $Pt_4CH_2^+$ with O_2 theoretically. In this work, an extensive relativistic density functional study has been carried out on the $Pt_4CH_2^+/O_2$ system. Considering the possible interactions between $Pt_4CH_2^+$ and O_2, the precursor structures involved in the reactions have been carefully determined first. Combining previous experimental observations with the theoretical calculations,[4b,9] the plausible low-energy pathways were contrived, and the corresponding relative energy profiles have been explored for the reaction of $Pt_4CH_2^+$ with O_2.

2. Computational Details

All calculations have been performed using the Amsterdam Density Functional (ADF) package.[11] In all calculations, the 1s orbitals for carbon, nitrogen, and oxygen atoms and the 1s−4f orbitals for platinum are kept frozen in the frozen core approximation. The orbitals for valence electrons of all elements are expanded within the triple-ζ Slater-type basis set augmented with two polarization functions. Frequency analyses have been carried out to assess the nature of stationary points. The zero-point energy corrections have been incorporated into the total electronic energies.

The zero-order regular approximation formalism (ZORA)[12] has been used to account for the relativistic effect without including the spin−orbit coupling.[13] Our previous calculations[5c] indicate that the ZORA treatment without the spin−orbit coupling on the CH_4/Pt_n^+ ($n = 2-4$) systems can predict reasonably qualitative results compared with experiments and provide a theoretical basis for understanding the anomalous behavior of Pt_4^+ in methane dehydrogenation. The PW91 exchange and correlation functionals[14] have been used throughout this work, and they have been verified to be reliable for the properties of the neutral and charged platinum clusters.[15] Our test calculations by the PW91 functional show that the dissociation energy of Pt_2 was somewhat overestimated by 0.5 eV without the spin−orbit coupling. If the spin−orbit coupling effect was taken into account in calculation, the predicted dissociation energy of Pt_2 at its ground state ($^3\Sigma_g^-$) is 3.31 eV, in good agreement with the latest experimental value of 3.14 eV.[16] In previous calculations,[17] the spin−orbit coupling effect was approximately estimated within ~10 kcal mol^{-1}. Since the spin flip was probably involved in transition-metal-mediated reactions,[18] different spin multiplicities of reactants have been considered.

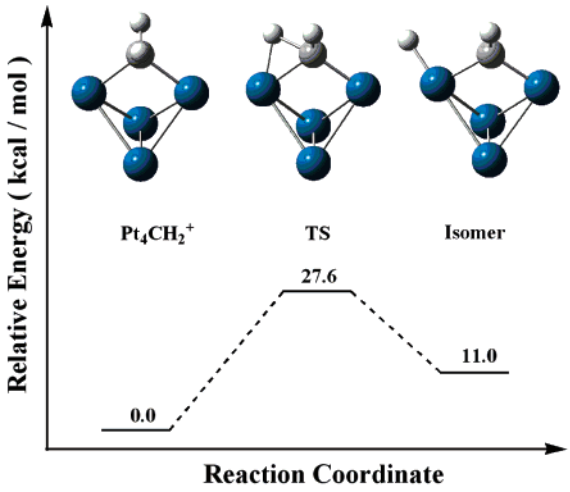

Figure 1. Relative energy profiles for isomerization of $Pt_4CH_2^+$.

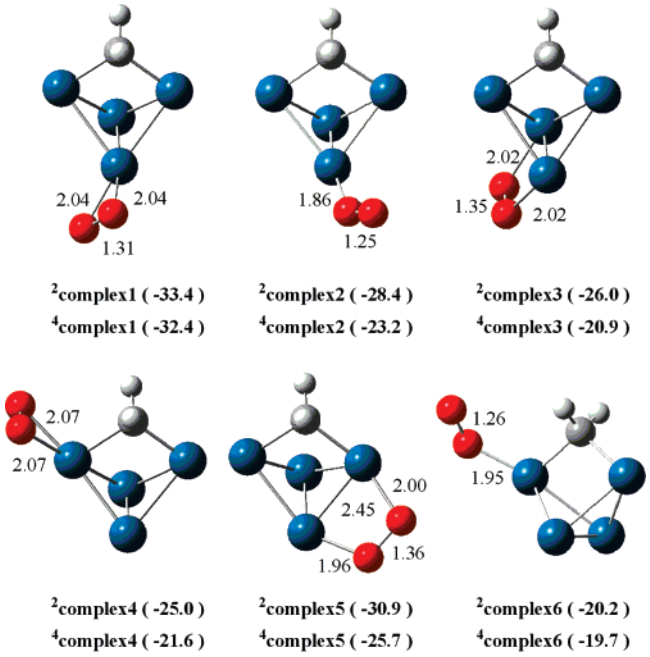

Figure 2. Optimized structures of $Pt_4CH_2(O_2)^+$ and calculated relative energies to the reactants of $Pt_4CH_2^+$ and O_2 (kcal mol^{-1}). Bond lengths are in angstroms.

3. Results and Discussion

A. Structures and Stabilities of $Pt_4CH_2^+$ and Its Complex with O_2. In previous study of methane dehydrogenation by the

(11) te Velde, G.; Bickelhaupt, F. M.; Baerends, E. J.; Guerra, C. F.; Gisbergen, S. J. A. V.; Snijders, J. G.; Ziegler, T. *J. Comput. Chem.* **2001**, *22*, 931.

(12) (a) van Lenthe, E.; Baerends, E. J.; Snijders, J. G. *J. Chem. Phys.* **1993**, *99*, 4597. (b) van Lenthe, E.; Baerends, E. J.; Snijders, J. G. *J. Chem. Phys.* **1994**, *101*, 9783. (c) van Lenthe, E.; Snijders, J. G.; Baerends, E. J. *J. Chem. Phys.* **1996**, *105*, 6505. (d) van Lenthe, E.; Ehlers, A. E.; Baerends, E. J. *J. Chem. Phys.* **1999**, *110*, 8943.

(13) (a) Pyykkö, P. *Chem. Rev.* **1988**, *88*, 563. (b) Schwarz, H. *Angew. Chem., Int. Ed.* **2003**, *42*, 4442. (c) Pyykkö, P. *Angew. Chem., Int. Ed.* **2004**, *43*, 4412. (d) Pyykkö, P. *Inorg. Chim. Acta* **2005**, *358*, 4113.

(14) (a) Perdew, J. P. *Phys. Rev. B* **1986**, *33*, 8822. (b) Perdew, J. P.; Chevary, J. A.; Vosko, S.; Jackson, K. A.; Pederson, M. R.; Singh, D. J.; Fiolhais, C. *Phys. Rev. B* **1992**, *46*, 6671.

(15) Fortunelli, A. *J. Mol. Struct. (THEOCHEM)* **1999**, *493*, 233.

(16) Airola, M. B.; Morse, M. D. *J. Chem. Phys.* **2002**, *116*, 1313.

(17) (a) Brönstrup, M.; Schröder, D.; Kretzschmar, I.; Schwarz, H.; Harvey, J. N. *J. Am. Chem. Soc.* **2001**, *123*, 142. (b) Zhang, X. G.; Armentrout, P. B. *J. Phys. Chem. A* **2003**, *107*, 8904. (c) Heinemann, C.; Koch, W.; Schwarz, H. *Chem. Phys. Lett.* **1995**, *245*, 509.

(18) (a) Shaik, S.; Danovich, D.; Fiedler, A.; Schröder, D.; Schwarz, H. *Helv. Chim. Acta* **1995**, *78*, 1393. (b) Danovich, D.; Shaik, S. *J. Am. Chem. Soc.* **1997**, *119*, 1773. (c) Schröder, D.; Shaik, S.; Schwarz, H. *Acc. Chem. Res.* **2000**, *33*, 139. (d) Schwarz, H. *Int. J. Mass Spectrom.* **2004**, *237*, 75.

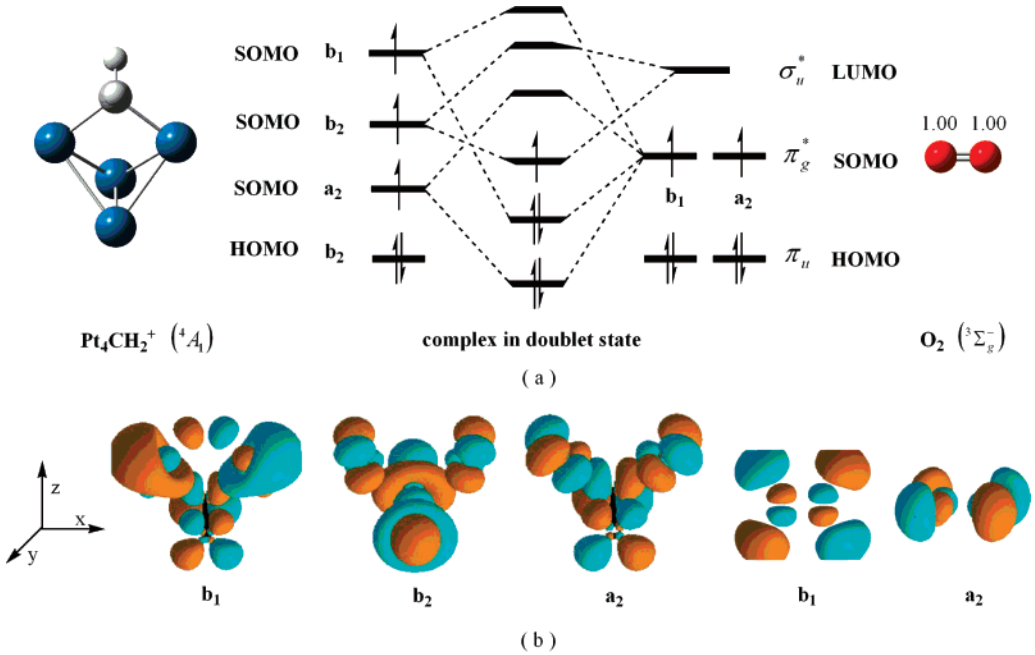

Figure 3. (a) Schematic illustration of the frontier orbital interactions between $Pt_4CH_2^+$ and O_2. (b) Contours of related SOMOs of $Pt_4CH_2^+$ and O_2.

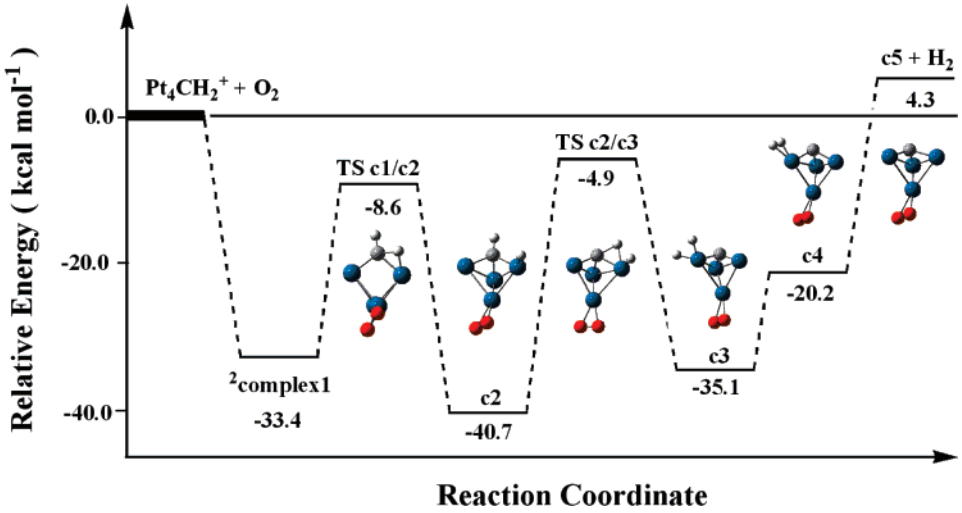

Figure 4. Relative energy profiles of dehydrogenation reaction of $Pt_4CH_2^+$ with O_2.

cluster Pt_4^+,[5c] the optimized ground state of the dehydrogenated product $Pt_4CH_2^+$ is $^4A_1$ with C_{2v} symmetry. The next low-energy doublet state is $^2B_2$, and it is less stable than the quartet ground state by 1.9 kcal mol^{-1}. Figure 1 shows that the further hydrogen transfer from the CH_2 moiety of $Pt_4CH_2^+$ to the vicinal platinum has a substantially high barrier of 27.6 kcal mol^{-1}, giving rise to a less stable isomer. Therefore, the isolated quartet $Pt_4CH_2^+$ has relatively high stability in the gas phase, and the bridging CH_2 moiety can be involved in further reactions with O_2, NH_3, and H_2O.[9]

Experimentally, the association of NH_3 and H_2O with $Pt_4CH_2^+$ may promote the dehydrogenation of the CH_2 moiety. The deuterium labeling experiments[9] have revealed that, in the reactions of $Pt_4CH_2^+$ with NH_3 and H_2O, the dehydrogenation exclusively occurs in the CH_2 moiety of $Pt_4CH_2^+$, and the corresponding reaction efficiencies for NH_3 and H_2O are 0.86 and 0.41, respectively. Koszinowski et al.[9] have ascribed such differences in reactivity to respective nucleophilicities of NH_3 and H_2O. Further calculations predict that the complexation energies for the formation of adducts $Pt_4CH_2(NH_3)^+$ and $Pt_4CH_2(H_2O)^+$ are 45.3 and 25.5 kcal mol^{-1}, respectively. The energy release from the complex $Pt_4CH_2(NH_3)^+$ is enough to surpass the barrier of the hydrogen transfer. However, for the adduct $Pt_4CH_2(H_2O)^+$, the releasing complexation energy of 25.5 kcal mol^{-1} is just comparable to the barrier, and thus the dehydrogenation efficiency is relatively low, as observed experimentally.

Figure 2 displays the optimized structure of the complex $Pt_4CH_2(O_2)^+$. The calculated energies of the doublet and quartet complexes in parentheses are relative to the energy sum of the ground states of $Pt_4CH_2^+$ and O_2. The superscripts **2** and **4** such as in structures **^{2}complex1** and **^{4}complex1** denote the doublet state and the quartet state, respectively. The calculations have shown that the structures of **^{2}complex1** and **^{4}complex1** with the side-on dioxygen are the most energy-favored coordination patterns, where the doublet state is slightly lower in energy than the quartet counterpart by 1.0 kcal mol^{-1}. The small doublet−quartet energy gap of 1.0 kcal mol^{-1} may give rise to the spin flip between the different spin states.[18c] The formation of the low-energy doublet structure can be rationalized through the

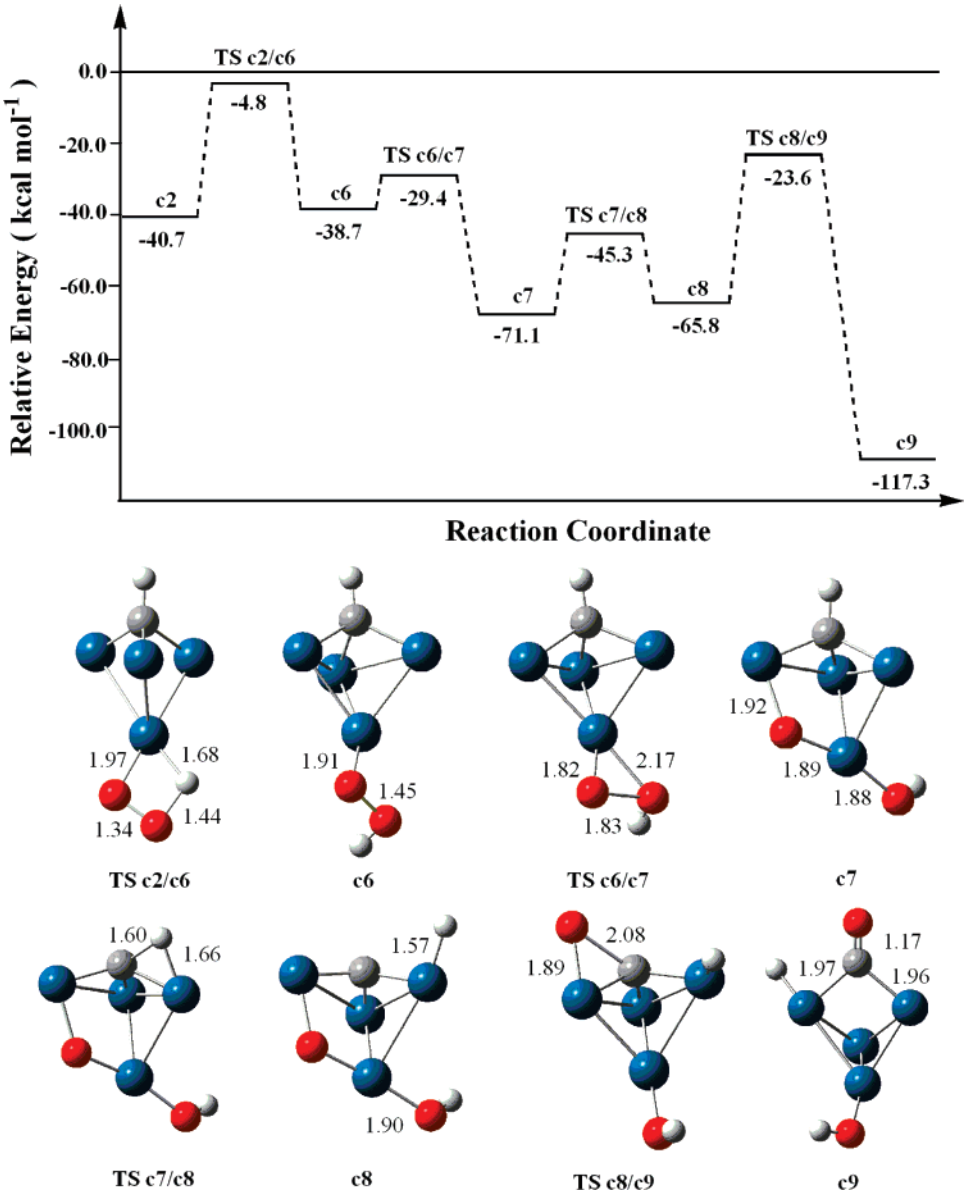

Figure 5. Relative energy profiles for the O−O bond activation and C−O bond coupling, as well as the corresponding structures of intermediates and transition states. Bond lengths are in angstroms.

visual frontier orbital theory and donor−acceptor interactions.[19] The schematic illustration for the frontier orbital interactions of $Pt_4CH_2^+$ with O_2 is depicted in Figure 3. As shown in Figure 3a, the symmetries of the singly occupied molecular obitals (SOMOs) of $Pt_4CH_2^+$ are b_1, b_2, and a_2, respectively. The degenerate antibonding π^* orbitals of O_2 have b_1 and a_2 symmetries under the C_{2v} point group. These electrons in b_1 and a_2 SOMOs of $Pt_4CH_2^+$ may couple with the two unpaired electrons in the symmetry-adaptation antibonding π^* orbitals of O_2 to form two bonding electron pairs in the doublet **^{2}complex1**. As Figure 3b displays, there are many possible local-orbital-phase adaptation patterns for the association of $Pt_4CH_2^+$ with O_2. Hence, the formed complexes exhibit distinct structural varieties as shown in Figure 2. Among these complexes, **^{2}complex1** in the doublet state is the lowest-energy species and it should be taken as the precursor of consecutive reactions of $Pt_4CH_2^+(O_2)$.

(19) (a) Fukui, K. *J. Phys. Chem.* **1970**, *74*, 4161. (b) Fukui, K. *Acc. Chem. Res.* **1981**, *14*, 363. (c) Dewar, M. J. S. *Bull. Soc. Chem. Fr.* **1951**, *18*, C71. (d) Chatt, J.; Duncanson, L. A. *J. Chem. Soc.* **1953**, 2939.

B. Mechanisms of Reactions of $Pt_4CH_2^+$ with O_2. In the present work, we proposed possible mechanisms for the reaction of $Pt_4CH_2^+$ with O_2, which are different from those for the reaction of $PtCH_2^+$ with O_2 suggested by Pavlov et al.[4b] Due to the presence of an sp^2-hybrid carbon atom in the carbene species $PtCH_2^+$, the direct C−O bond coupling between $PtCH_2^+$ and O_2 is available. However, the direct attack of metal-bound dioxygen toward the carbon atom is not favorable energetically in an end-on complex $Pt_4CH_2^+(O_2)$, in which the sp^3-hybrid carbon atoms in the CH_2 moiety are coordinatedly saturated. The formation of the lowest-energy precursor **^{2}complex1** has an exothermicity of 33.4 kcal mol^{-1}, and the energy release may drive the hydrogen transfer from CH_2 to metal atoms in **^{2}complex1**, which was verified to be the most favorable elementary step energetically in preliminary calculations.

Since the presence of multi-metal centers makes the reaction channels become much complicated, it is important to contrive subsequent reaction processes. In the reaction of $PtCH_2^+$ with O_2,[4b] it was noted that the branch channels to products of H_2O/CO and HCOOH request the occurrence of the O−O bond

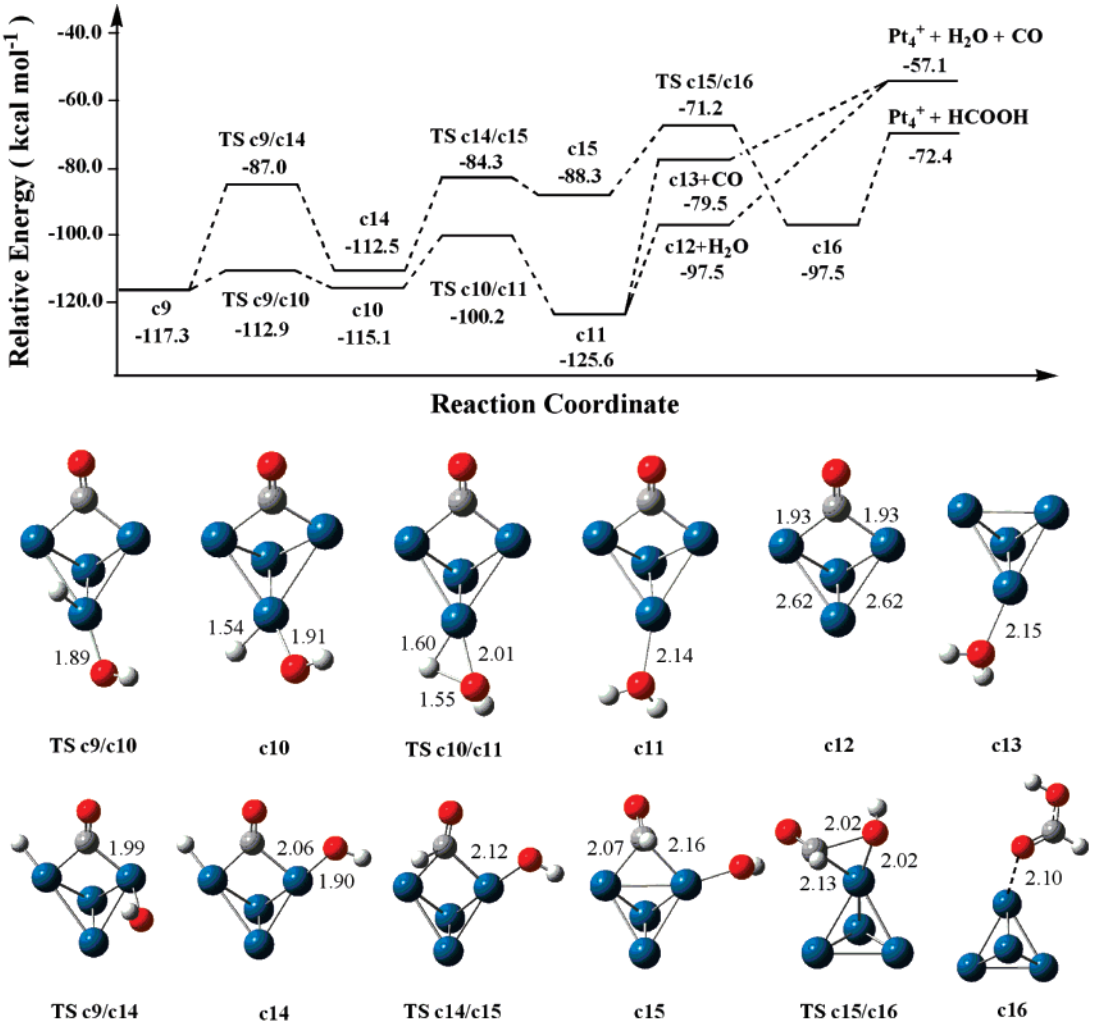

Figure 6. Relative energy profiles along the channels to H_2O/CO and HCOOH and the corresponding structures of intermediates and transition states. Bond lengths are in angstroms.

activation of dioxygen and the O−H bond coupling, while the generation of H_2/CO_2 does not. On the basis of the analysis of product varieties, two types of reaction mechanisms for the loss of H_2 and the oxidation of CH_2 to H_2O/CO or HCOOH have been considered for the reaction of $Pt_4CH_2^+$ with O_2.

1. Reaction Pathway to Elimination of H_2. Figure 4 presents the relative energy profiles of dehydrogenation of $Pt_4CH_2^+$ with O_2, as well as corresponding structures of intermediates and transition states. The ground-state reactants of $Pt_4CH_2^+$ and O_2 serve as the reference state in determining the relative energetics. As Figure 4 shows, the formation of ^{2}**complex1** releases energy of 33.4 kcal mol^{-1}, which is enough to overcome the barrier of 24.8 kcal mol^{-1} for the first C−H bond activation of the CH_2 moiety in ^{2}**complex1**. Through the transition state **TS c1/c2**, the precursor ^{2}**complex1** evolves to a more stable hydride **c2**. Followed by the second C−H bond activation via the transition state **TS c2/c3**, a dihydride **c3** forms with a barrier of 35.8 kcal mol^{-1}, and the transition state **TS c2/c3** is slightly lower in energy than the reactants by 4.9 kcal mol^{-1}. The dihydride **c3** evolves into a dihydrogen complex **c4** with an endothermicity of 20.2 kcal mol^{-1}. There is no transition state to be located between **c3** and **c4** due to strong interactions of dihydrogen with the metal cluster.[5c] Finally, the liberation of H_2 from **c4** requires 24.5 kcal mol^{-1} to yield the products **c5**. The overall reaction of dehydrogenation is predicted to be endothermic by 4.3 kcal mol^{-1}, and the Gibbs free energy of reaction $\Delta G = 5.4$ kcal mol^{-1} (at 298.15 K). The calculation results indicate the dehydrogenation of $Pt_4CH_2^+$ with O_2 is likely to occur in the gas phase. However, this channel to loss of H_2 is less efficient thermodynamically in comparison with other branch channels (vide infra), and thus the further reaction to yield CO_2 has not been explored here.

2. Reaction Pathway to H_2O/CO. In the dehydrogenation route as shown in Figure 4, the most stable intermediate **c2** is a local minimum on the potential energy surface, and as a precursor it can be involved in other reaction channels. Here we explored the reaction channel to H_2O and CO from the lowest-energy intermediate **c2**, where the elementary reactions steps of O−O bond activation as well as C−O and O−H bond couplings are involved. Figure 5 displays the relative energy profiles and corresponding structures of intermediates and transition states along this reaction channel.

As Figure 5 displays, the hydrogen transfer from metal to dioxygen in **c2** forms an intermediate **c6** via a four-membered ring transition state **TS c2/c6** with a barrier of 35.9 kcal mol^{-1}. The Pt−H and O−O bond lengths of **TS c2/c6** are 1.68 and 1.34 Å, respectively, and the O−OH bond length in **c6** is 1.45 Å. Followed by the O−O bond fission, the intermediate **c6** proceeds to a more stable intermediate **c7** with a Pt-bound hydroxyl. The formation of the intermediate **c7** has a remarkable exothermicity of 71.1 kcal mol^{-1} relative to the reaction entrance in Figure 4, which may facilitate the further hydrogen transfer. The second C−H bond activation leads to a less stable intermediate **c8** with a barrier of 25.8 kcal mol^{-1}. The C−O

bond coupling in **c8** via the transition state **TS c8/c9** has a substantial barrier of 42.2 kcal mol^{-1}, generating the primary product **c9** with the bridged μ_2-CO structure. The overall process is exothermic by 76.6 kcal mol^{-1} relative to **c2**.

The metal-bound hydrogen, hydroxyl, and carbonyl in **c9** can undergo consecutive rearrangements to yield the products of H_2O/CO or HCOOH. Possible mechanisms for subsequent branch channels and optimized structures of transition states and intermediates in reaction are displayed in Figure 6. In **c9**, the hydrogen migration results in an intermediate **c10**. Followed by the coupling of hydrogen with hydroxyl, the more stable complex **c11** with the Pt-bound water is formed with a barrier of 15 kcal mol^{-1}. The formation of **c11** has the enormous exothermicity of 125.6 kcal mol^{-1} relative to $Pt_4CH_2^+ + O_2$. Such striking energy release may cause the elimination of H_2O or CO from complex **c11**, yielding primary products **c13** or **c12** and ultimate products Pt_4^+/H_2O/CO. Calculations indicate that the release of water from **c11** requires 28.1 kcal mol^{-1}, while the liberation of CO needs 46.1 kcal mol^{-1}. The overall channel to the products H_2O/CO has an exothermicity of 57.1 kcal mol^{-1} and free energy of reaction $\Delta G = 66.2$ kcal mol^{-1} relative to the reaction entrance $Pt_4CH_2^+ + O_2$.

3. Reaction Pathway to HCOOH. Another branch channel to the products of Pt_4^+ and HCOOH starting from **c9** is also shown in Figure 6. Obviously, the formation of the formic acid molecule requires the consecutive couplings of the metal-bound hydrogen and hydroxyl with the carbonyl group in the intermediate **c9**. First, the hydroxyl transfer in **c9** yields **c14** with the activation barrier of 30.3 kcal mol^{-1}. The intermediate **c14** evolves to **c16** through transition states **TS c14/c15** and **TS c15/c16** with barriers of 28.2 and 17.1 kcal mol^{-1}, respectively. The C−H and C−OH bond couplings are involved in the formation of **c16**. The structure of **c16** can be viewed as the molecular complex of the cationic cluster Pt_4^+ with the neutral formic acid molecule though the charge−dipole interactions. The final elimination of formic acid from **c16** requires the energy of 25.1 kcal mol^{-1}.

As Figure 6 displays, predicted relative energy profiles for the branch channels to H_2O/CO and HCOOH indicate that the initial elementary steps for the products H_2O/CO are more favorable energetically, whereas the ultimate product HCOOH is more stable than H_2O/CO by 15.3 kcal mol^{-1}. The calculated Gibbs free energy of reaction ΔG for the formation of HCOOH is 73.5 kcal mol^{-1}, 7.3 kcal mol^{-1} lower than that of H_2O/CO. Therefore, both branch channels should be competitive in reaction, and the mixtures of H_2O/CO and HCOOH might be the primary components of neutral products [C, H_2, O_2] observed in experiments.

In contrast to $Pt_4CH_2^+$, the smaller cluster $Pt_2CH_2^+$ is unreactive and $Pt_3CH_2^+$ is much less efficient in the reaction with O_2.[9] To have an insight into the size dependence of reactivity, further calculations on the reactions of $Pt_nCH_2^+$ ($n = 2,3$) with O_2 have been performed, and detailed results are available in the Supporting Information. Calculations indicate that such remarkable reactivity may arise from the distinct frontier orbital interactions as well as possible spin flip. For example, the inertia of $Pt_2CH_2^+$ toward O_2 can be ascribed to the violation of the symmetry-adaptation rule for frontier orbital interactions. Furthermore, the large energy splitting between the doublet−quartet states of the side-on complex of $Pt_2CH_2^+$ with O_2 may prevent the spin flip and the formation of a low-energy doublet precursor to subsequent reactions. As shown in Figures 2 and 3, the symmetry-adaptation frontier orbitals between $Pt_4CH_2^+$ and O_2 can effectively admix to form the more stable complex as the precursor of reaction. The small energy gap of 1 kcal mol^{-1} between ^{2}**complex1** and ^{4}**complex1** (see Figure 2) makes the spin transition facile. The predicted relative energetic for the dehydrogenation channel in the reaction of $Pt_nCH_2^+$ ($n = 2-4$) with O_2 shows that the larger cluster $Pt_4CH_2^+$ has relatively high reactivity.

4. Conclusions

Possible mechanisms for the reaction of $Pt_4CH_2^+$ with O_2 have been studied by the relativistic density functional theory method. Predicted thermodynamic values indicate that the dehydrogenation branch channel in the reaction is less efficient with the Gibbs free energy of reaction $\Delta G = 5.4$ kcal mol^{-1}, whereas the branch channels to products H_2O/CO and HCOOH are quite favorable thermodynamically. In the energy-favored processes to H_2O/CO and HCOOH, the corresponding overall Gibbs free energies are −66.2 and −73.5 kcal mol^{-1}, respectively, and both branch channels might be competitive in consideration of balance between dynamic and thermodynamic aspects. The intermediate $[(\mu_2\text{-CO})(H)Pt_4(OH)]^+$ (**c9**) was predicted to be the important precursor for both channels to H_2O/CO and HCOOH, and the release of CO in **c9** is the key step for the formation of H_2O/CO. The calculation results provide a basis for understanding the size dependence of reactivity for $Pt_nCH_2^+$ ($n = 2-4$).

Acknowledgment. We acknowledge financial support from the National Science Foundation of China (Grants 20673087, 20733002, 20473062, and 20423002), and the Ministry of Science and Technology (Grant 2004CB719902).

Supporting Information Available: Investigation and discussion of reactions of $Pt_nCH_2^+$ ($n = 2,3$) with O_2. This material is available free of charge via the Internet at http://pubs.acs.org.

OM700288A